

Top pair production near threshold in e^+e^- collisions

M. Beneke (TU München)

MIAPP LHC programme, Top-quark Physics Day
Munich, 11 August 2014

Outline

- Introduction and theoretical framework
- Top production near threshold in e^+e^- collisions – Third-order QCD effects and parameter variations

MB, Kiyo, Schuller, 1312.4791 [hep-ph] and in preparation;

MB, Piclum, Rauh, 1312.4792 [hep-ph];

MB, ..., Steinhauser, in preparation; MB, Piclum, Rauh, in progress.

- Beyond QCD – Non-resonant effects

MB, Jantzen, Ruiz-Femenia 1004.2188 [hep-ph];

Jantzen, Ruiz-Femenia 1307.4337 [hep-ph]



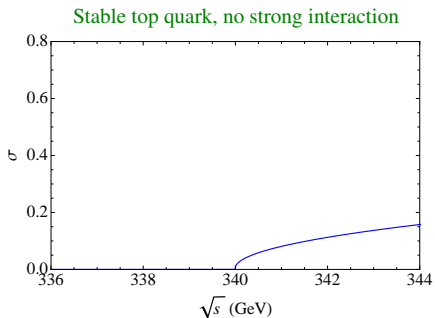
Top quark parameters from $e^+e^- \rightarrow t\bar{t}$ near threshold

- Ultra-precise mass measurement ($\delta m_t < 100$ MeV)
 - for the Particle Data Book
 - vacuum stability
 - lepton-quark unification

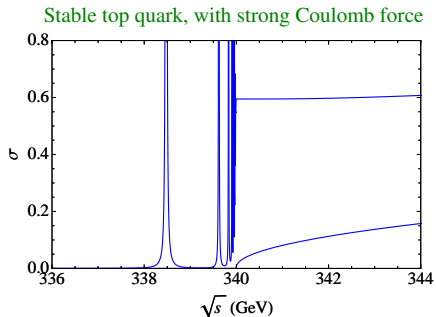
Enough motivation to perform a really nice (challenging) calculation.

- Direct spectroscopic width measurement
- Sensitivity to top-Yukawa coupling

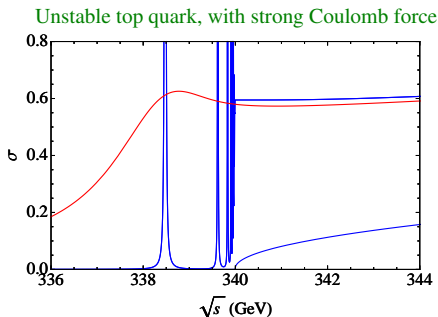
Ultra-precise mass measurement
Unique QCD dynamics



Ultra-precise mass measurement
Unique QCD dynamics

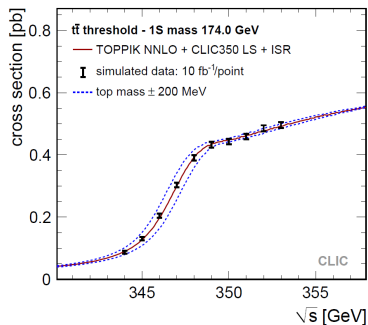


Ultra-precise mass measurement
Unique QCD dynamics



Smallest structure in particle physics known to exist (10^{-17} m).
Direct “spectroscopic” mass and width measurement.

Additional smearing of the resonance due to beam luminosity spectrum (collider-specific) and ISR



Most recent study for ILC/CLIC [Seidel, Simon, Tesai, Poss, 2013] assumes 10 fb^{-1} at 10 points.

$$[\delta m_t]_{\text{thr}} = 27 \text{ MeV} \quad [\text{simultaneous fit of } \alpha_s]$$

Non-perturbative but weak coupling. Expansion in α_s and $v = \sqrt{\frac{E}{m}} = \sqrt{\frac{\sqrt{q^2} - 2m_t}{m_t}}$, while $\alpha_s/v = O(1)$

$$R \sim v \sum_k \left(\frac{\alpha_s}{v} \right)^k \cdot \left\{ 1 \text{ (LO)}; \alpha_s, v \text{ (NLO)}; \alpha_s^2, \alpha_s v, v^2 \text{ (NNLO)}; \dots \right\}$$

$$(q_\mu q_\nu - q^2 g_{\mu\nu}) \Pi(q^2) = i \int d^4x e^{iq \cdot x} \langle 0 | T(j_\mu(x) j_\nu(0)) | 0 \rangle, \quad j^\mu(x) = [\bar{Q} \gamma^\mu (\gamma_5) Q](x)$$

Summation through Schrödinger equation.

$$\text{Im } \Pi(E) = \underbrace{\frac{N_c}{2m^2} \sum_{n=1}^{\infty} Z_n \times \pi \delta(E_n - E)}_{\text{bound states}} + \Theta(E) \underbrace{\text{Im } \Pi(E)_{\text{cont}}}_{\text{continuum}}$$

$$R \equiv \frac{\sigma_{e^+e^- \rightarrow WWb\bar{b}X}}{\sigma_0} = 12\pi e_t^2 \text{Im } \Pi(E + i\Gamma_t) + \text{non-resonant}$$

Non-relativistic effective field theory and threshold expansion (defines the matching procedure!)
See [arXiv:1312.4791](https://arxiv.org/abs/1312.4791) [hep-ph]

Relevant scales: $m_t \approx 175$ GeV (**hard**), $m_t \alpha_s \approx 30$ GeV (**soft, potential**) and the **ultrasoft scale (us)** $m_t \alpha_s^2 \approx 2$ GeV.

$$\mathcal{L}_{\text{QCD}} [Q(h, s, p), g(h, s, p, us)] \quad \mu > m_t$$



$$\mathcal{L}_{\text{PNRQCD}} [Q(p), g(us)] \quad \mu < m_t v$$

See mult-loop fixed-order calculations to match PNRQCD, then perturbation theory in Coulomb background in PNRQCD. Can be extended systematically to any order. 3rd order is current technological limit.

$$\Pi^{(v)}(q^2) = \frac{N_c}{2m^2} c_v \left[c_v - \frac{E}{m} \left(c_v + \frac{d_v}{3} \right) \right] G(E) + \dots$$

$$G(E) = \frac{i}{2N_c(d-1)} \int d^d x e^{iEx^0} \langle 0 | T([\chi^\dagger \sigma^i \psi](x) [\psi^\dagger \sigma^i \chi](0)) | 0 \rangle_{\text{PNRQCD}},$$

Integrating out soft fluctuations results in a spatially non-local effective Lagrangian since $[k^i]_{\text{soft}} \sim [k^i]_{\text{pot}}$.

$$\begin{aligned}\mathcal{L}_{\text{PNRQCD}} = & \psi^\dagger \left(iD_0 + i\frac{\Gamma_t}{2} + \frac{\partial^2}{2m} + \frac{\partial^4}{8m^3} \right) \psi + \chi^\dagger \left(iD_0 - i\frac{\Gamma_t}{2} - \frac{\partial^2}{2m} - \frac{\partial^4}{8m^3} \right) \chi \\ & + \int d^{d-1} \mathbf{r} \left[\psi^\dagger \psi \right] (x + \mathbf{r}) \left(-\frac{\alpha_s C_F}{r} + \delta V(r, \partial) \right) \left[\chi^\dagger \chi \right] (x) \\ & - g_s \psi^\dagger(x) \mathbf{x} \mathbf{E}(t, \mathbf{0}) \psi(x) - g_s \chi^\dagger(x) \mathbf{x} \mathbf{E}(t, \mathbf{0}) \chi(x)\end{aligned}$$

- The leading-order Coulomb potential is part of the unperturbed Lagrangian. The asymptotic states correspond to the composite field $[\psi^\dagger \chi](\mathbf{R}, \mathbf{r})$ with free propagation in the cms coordinate. **The propagation in the relative coordinate is determined by the Coulomb Green function $G_c^{(1)}(\mathbf{r}, \mathbf{r}'; E)$**
- Perturbations consist of **kinetic energy corrections, perturbation potentials, and ultrasoft gluon interactions.**

- Bound state quantities (S-wave)

- E_n – Kniehl, Penin, Smirnov, Steinhauser (2002); MB, Kiyo, Schuller (2005); Penin, Sminrov, Steinhauser (2005)
- $|\psi_n(0)|^2$ – MB, Kiyo, Schuller (2007); MB, Kiyo, Penin (2007)

- Matching coefficients

- a_3 – Anzai, Kiyo, Sumino (2009); Smirnov, Sminrov, Steinhauser (2009)
- c_3 – Marquard, Piclum, Seidel, Steinhauser (2013) [2009]

- Continuum (PNRQCD correlation function)

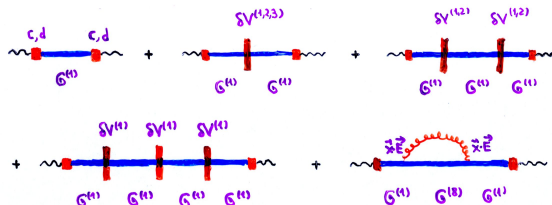
- ultrasoft – MB, Kiyo (2008)
- potential – MB, Kiyo, Schuller, in preparation (2014) [2007]
- P-wave – MB, Piclum, Rauh (2013)

Note: logarithmically enhanced 3rd order terms known before or resummed [Hoang et al. 2001-2013; Pineda et al. 2002-2007]

2nd order available since end of 1990s.

The NNNLO contribution to the PNRQCD correlation function is

$$G^{(3)} = -G_c^{(1)} \delta V_1 G_c^{(1)} \delta V_1 G_c^{(1)} \delta V_1 G_c^{(1)} + 2G_c^{(1)} \delta V_1 G_c^{(1)} \delta V_2 G_c^{(1)} - G_c^{(1)} \delta V_3 G_c^{(1)} + \delta G_{\text{us}}$$



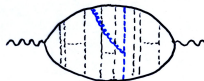
where

$$G_c^{(1,8)}(\mathbf{r}, \mathbf{r}', E) = \frac{my}{2\pi} e^{-y(r+r')} \sum_{l=0}^{\infty} (2l+1)(2yr)^l (2yr')^l P_l \left(\frac{\mathbf{r} \cdot \mathbf{r}'}{rr'} \right) \sum_{s=0}^{\infty} \frac{s! L_s^{(2l+1)}(2yr) L_s^{(2l+1)}(2yr')}{(s+2l+1)!(s+l+1-\lambda)}$$

$$y = \sqrt{-m(E+i\epsilon)}, \lambda = \frac{m\alpha_s}{2y} \times \{C_F \text{ (singlet); } C_F - C_A/2 \text{ (octet)}\}$$

For singlet need only $l = 0$, for octet only $l = 1$.

The ultrasoft contribution is ($D = d - 1$)



$$\delta G_{\text{us}} = (-i)(ig_s)^2 C_F \int \frac{d^d k}{(2\pi)^d} \frac{-i}{k^2} \left(\frac{k^i k^j}{k_0^2} - \delta^{ij} \right) \int \prod_{n=1}^6 \frac{d^D p_n}{(2\pi)^D} i\tilde{G}^{(1)}(p_1, p_2; E) i\tilde{G}^{(8)}(p_3, p_4; E + k^0) i\tilde{G}^{(1)}(p_5, p_6; E)$$

$$\times i \left[\frac{2p_3^i}{m_t} (2\pi)^D \delta^{(D)}(p_3 - p_2) + (ig_s)^2 \frac{C_A}{2} \frac{2(p_2 - p_3)^i}{(p_2 - p_3)^4} \right] i \left[-\frac{2p_4^j}{m_t} (2\pi)^D \delta^{(D)}(p_4 - p_5) + (ig_s)^2 \frac{C_A}{2} \frac{2(p_4 - p_5)^j}{(p_4 - p_5)^4} \right]$$

- In position space only three instead of seven integrations, but the integrals are divergent and the $1/\epsilon$ poles must be extracted in momentum space.
- The Coulomb Green functions are not known in D dimensions.
- UV divergence in the ultrasoft k integral is related to potentials and the derivative current. UV divergence in potential p_i integrals are related to the non-relativistic vector current.
- **Strategy: identify divergent subgraphs, calculate them in D dim. momentum space, combine with counterterm and perform remaining integrations in three dimensions.**

Example of divergence extraction:

$$\begin{aligned}
 [G_{\text{nC}}^{(3)}]_{\text{div}} = & \left[-\frac{1}{\epsilon^2} \left(\frac{7}{72} C_F^2 + \frac{2}{9} C_A^2 + \frac{23}{48} C_A C_F + \beta_0 \left(\frac{C_A}{24} + \frac{C_F}{36} \right) \right) \right. \\
 & - \frac{1}{\epsilon} \left\{ \left(\frac{11}{24} - \frac{L_m}{12} \right) C_F^2 + \left(\frac{427}{324} - \frac{4 \ln 2}{3} - \frac{L_m}{8} \right) C_A C_F - \left(\frac{5}{216} + \frac{2 \ln 2}{3} \right) C_A^2 \right. \\
 & \left. \left. + \left(\frac{C_A}{24} + \frac{C_F}{54} \right) \beta_0 - \left(\frac{1}{30} - \frac{29 n_f}{162} \right) C_F T_F + \frac{49}{216} C_A T_F n_f \right\} \right] \frac{\alpha_s^3 C_F}{\pi} \langle 0 | \hat{G}_c^{(1)} | 0 \rangle \\
 & - \left[\frac{1}{4} C_A + \frac{1}{6} C_F \right] \frac{\alpha_s^2 C_F}{\epsilon} \langle 0 | \hat{G}_c^{(1)} \delta V_1 \hat{G}_c^{(1)} | 0 \rangle \quad (L_m = \ln(\mu/m))
 \end{aligned}$$

The ultrasoft contribution is more complicated. Extract the vertex divergence by subtracting three-loop vertex diagrams at zero momentum:

The remaining finite parts are expressed as (multiple) sums of Gamma functions, PolyGamma functions, Hypergeometric functions in case of potential corrections and numerical integrations in case of the ultrasoft correction. Pole parts are cancelled analytically.

I. Top production near threshold in e^+e^- collisions – QCD effects and parameter variations

MB, Kiyo, Schuller, 1312.4791 [hep-ph] and in preparation;

MB, ..., Steinhauser, in preparation (third-order QCD);

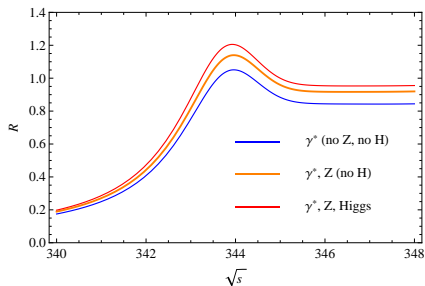
MB, Rauh, Piclum, in preparation (Higgs, top-Yukawa interaction)

- **Mass definition:** Potential-subtracted mass [MB, 1998]

$$m_{\text{PS}}(\mu_f) \equiv m_{\text{pole}} + \frac{1}{2} \int_{|\vec{q}| < \mu_f} \frac{d^3\vec{q}}{(2\pi)^3} \tilde{V}_{\text{Coulomb}}(\vec{q})$$

Cancellation of large perturbative contributions from the IR. In the following:

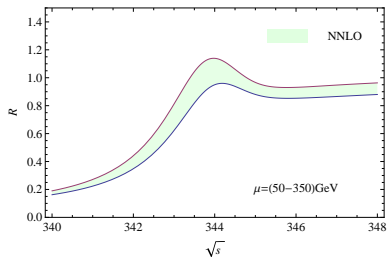
$$m_{t,\text{PS}}(20 \text{ GeV}) = 171.5 \text{ GeV.}$$



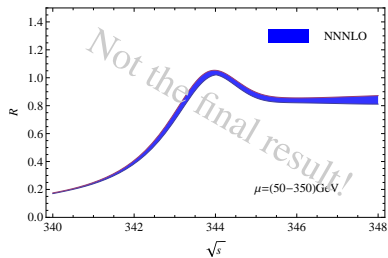
QCD at 3rd order + P-wave (Z only) + Higgs at NLO \simeq NNNLO QCD

Cross section near threshold, from 2nd to 3rd order

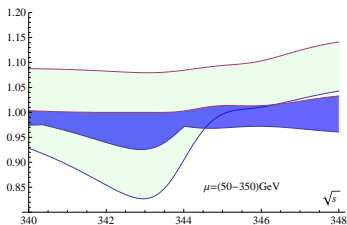
[MB, Signer, Smirnov, 1999]

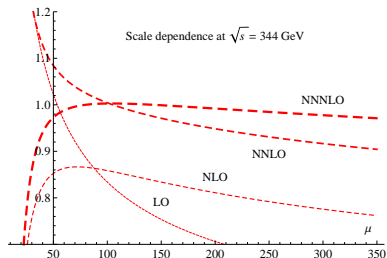


[MB, Kiyo, Schuller; MB ... Steinhauser, in progress]



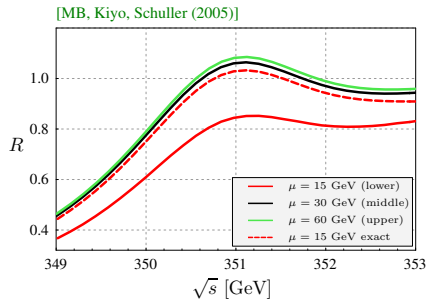
$$m_{t,\text{PS}}(20 \text{ GeV}) = 171.5 \text{ GeV}, \Gamma_t = 1.33 \text{ GeV}$$





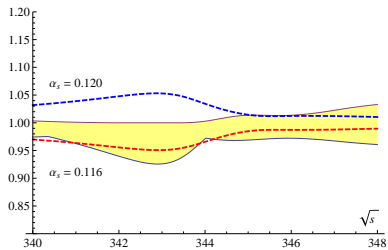
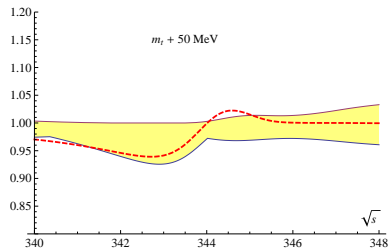
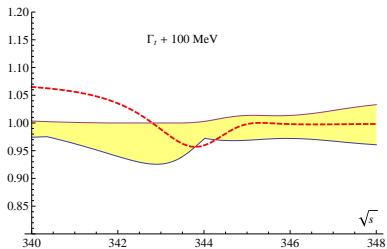
No convergence for $\mu \lesssim 50$ GeV.

Compare recent NNLO+(N)NLL analysis
[Hoang, Stahlhofen, 2013]



Coulomb corrections only (for $m_{t,PS} = 175$ GeV, $\Gamma_t = 1.5$ GeV). Scale dependence at third order and exact solution.

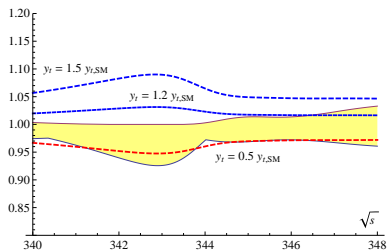
Parameter dependence



Count $\lambda_t = y_t^2/(4\pi)$ as electroweak coupling, i.e. $\lambda_t \sim \alpha_s^2 \sim v^2$ and $m_H \sim m_t$.

NNLO – 1-loop correction to vector-current matching

N3LO – Mixed 2-loop Higgs-QCD correction to vector-current matching [Eiras, Steinhauser, 2006]
Single insertion of Higgs-exchange tree-level potential into Coulomb Green function. In this order, the potential is local $y_t^2/m_H^2 \times \delta^{(3)}(\vec{r})$. [MB, Piclum, Rauh]



II. Non-resonant, finite-width, P-wave effects

MB, Piclum, Rauh, 1312.4792 [hep-ph];

MB, Jantzen, Ruiz-Femenia, 1004.2188 [hep-ph];

Jantzen, Ruiz-Femenia 1307.4337 [hep-ph]

Finite-width divergences and “electroweak effects”

The QCD-only result usually discussed is far from reality

- **Finite-width divergences** (overall log divergence, already at NNLO):

$$[\delta G(E)]_{\text{overall}} \propto \frac{\alpha_s}{\epsilon} \cdot E$$



Since $E = \sqrt{s} - 2m_t + i\Gamma$, the divergence survives in the imaginary part:

$$\text{Im} [\delta G(E)]_{\text{overall}} \propto m_t \times \frac{\alpha_s \alpha_{ew}}{\epsilon}$$

- **Electroweak effect. Must consider $e^+e^- \rightarrow W^+W^-b\bar{b}$.**

$$\sigma_{e^+e^- \rightarrow W^+W^-b\bar{b}} = \underbrace{\sigma_{e^+e^- \rightarrow [t\bar{t}]_{\text{res}}}(\mu_w)}_{\text{pure (PNR)QCD}} + \sigma_{e^+e^- \rightarrow W^+W^-b\bar{b}_{\text{nonres}}}(\mu_w)$$

Non-resonant starts at NLO (overall linear divergence) [MB, Jantzen, Ruiz-Femenia, 2010; Penin, Piclum, 2011]. Finite-width scale dep must cancel. Need consistent dim reg calculation.

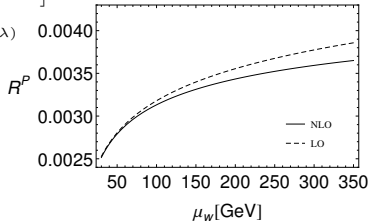
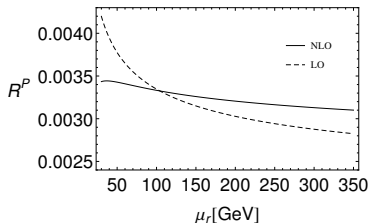
P-wave contribution at NLO (N3LO for total cross section)

$$R = 12\pi \operatorname{Im} \left[e_r^2 \Pi^{(v)}(q^2) - \frac{2q^2}{q^2 - M_Z^2} v_e v_r e_r \Pi^{(v)}(q^2) + \left(\frac{q^2}{q^2 - M_Z^2} \right)^2 (v_e^2 + a_e^2)(v_r^2 \Pi^{(v)}(q^2) + a_r^2 \Pi^{(a)}(q^2)) \right]$$

$$\begin{aligned} \delta_1 G^P(E) = & -\frac{m_r^4 \alpha_s^4 C_F^3}{64\pi^2 \lambda^2} \\ & \times \left\{ \beta_0 \left[\left(-\frac{1}{12\epsilon^2} + \frac{59}{9} + \frac{5\pi^2}{72} + 4L_\lambda' + 2L_\lambda' L_\lambda'' - (L_\lambda'')^2 \right) + (9 + 6L_\lambda') \lambda \right. \right. \\ & + \left(\frac{3}{40\epsilon^2} + \frac{1}{20\epsilon} - \frac{344}{15} - \frac{\pi^2}{8} - \frac{21}{2} L_\lambda' + \frac{1}{2} L_\lambda'' - 6L_\lambda' L_\lambda' + 3(L_\lambda'')^2 \right) \lambda^2 \\ & + [-4 - 6\lambda + 10\lambda^2 + 2(3\lambda^2 - 1)L_\lambda'] \hat{\psi}(2 - \lambda) \\ & + (\lambda - \lambda^3) \left[\psi_1(2 - \lambda) \left(\frac{22}{3} + 2L_\lambda' - 2\hat{\psi}(2 - \lambda) \right) + \psi_2(2 - \lambda) \right] \\ & \left. + (3\lambda^2 - 1) \left[3\psi_1(2 - \lambda) - \hat{\psi}(2 - \lambda)^2 \right] + \frac{3}{4 - 2\lambda} {}_4F_3(1, 1, 4, 4; 5, 5, 3 - \lambda; 1) \right] \\ & + a_1(\epsilon) \left[\frac{1}{6\epsilon} + 2 + L_\lambda'' + 3\lambda - \left(\frac{3}{10\epsilon} + \frac{26}{5} + 3L_\lambda'' \right) \lambda^2 + (3\lambda^2 - 1) \hat{\psi}(2 - \lambda) \right. \\ & \left. + (\lambda - \lambda^3) \psi_1(2 - \lambda) \right] \left. \right\}. \end{aligned}$$

[MB, Piclum, Rauh 2013]

Earlier numerical, non-dim reg result [Penin, Pivovarov, 1999]



At 3rd order QCD effects under control. Then

- $\sigma_{e^+e^- \rightarrow W^+W^-b\bar{b}_{\text{nonres}}}(\mu_w)$ to (at least) NNLO in consistent scheme. Mostly inclusive.

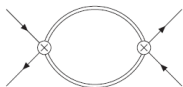
NLO [MB, Jantzen, Ruiz-Femenia, 2010; Penin, Piclum, 2011]

Partial results only at NNLO [Hoang, Reisser, Ruiz-Femenia, 2010; Jantzen, Ruiz-Femenia, 2013]

- QED effects (from NLO) [Pineda, Signer, 2006; MB, Jantzen, Ruiz-Femenia, 2010]
- Electroweak matching coefficients absorptive parts [Hoang, Reisser, 2004]
- Initial state radiation (formalism in MB, Falgari, Schwinn, Signer, Zanderighi, 2007).
- Higgs contributions [Eiras, Steinhauser, 2006]

Finally, need four-loop (formally even five-loop) relation between the pole and the $\overline{\text{MS}}$ mass to convert the precise value for the PS mass to an equally precise value of the $\overline{\text{MS}}$ mass.

Unstable particle EFT provides a systematic expansion of the amplitude in powers of Γ/m .



Resonant contributions

Production of an on-shell, non-relativistic $\bar{t}t$ pair and subsequent decay $t \rightarrow W^+ b$. Effective non-relativistic propagator contains on-shell width.



Non-resonant contributions

All-hard region. Off-shell lines. Full theory diagrams expanded around $s = 4m_t^2$. No width in propagators.

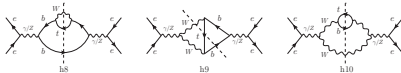
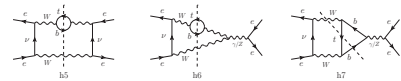
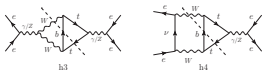
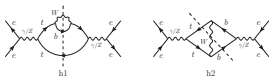
$$i\mathcal{A} = \sum_{k,l} C_p^{(k)} C_p^{(l)} \int d^4x \langle e^- e^+ | T [i\mathcal{O}_p^{(k)\dagger}(0) i\mathcal{O}_p^{(l)}(x)] | e^- e^+ \rangle + \sum_k C_{4e}^{(k)} \langle e^- e^+ | i\mathcal{O}_{4e}^{(k)}(0) | e^- e^+ \rangle$$

$$\mathcal{O}_p^{(v,a)} = \bar{e}_{c_2} \gamma_i (\gamma_5) e_{c_1} \psi_t^\dagger \sigma^i \chi_t$$

$$\mathcal{O}_{4e}^{(k)} = \bar{e}_{c_1} \Gamma_1 e_{c_2} \bar{e}_{c_2} \Gamma_2 e_{c_1},$$

$$\sigma_{\text{non-res}} = \frac{1}{s} \sum_k \text{Im} [C_{4e}^{(k)}] \langle e^- e^+ | i\mathcal{O}_{4e}^{(k)}(0) | e^- e^+ \rangle$$

Separately divergent and factorization (“finite-width”) scale-dependent.



$$\int_{\Delta^2}^{m_t^2} dp_t^2 (m_t^2 - p_t^2)^{\frac{d-3}{2}} H_i \left(\frac{p_t^2}{m_t^2}, \frac{M_W^2}{m_t^2} \right)$$

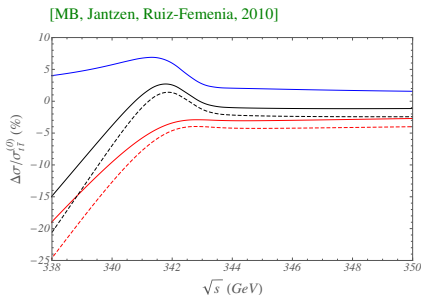
$$p_t^2 \equiv (p_b + p_{W^+})^2$$

$$H_1 \left(\frac{p_t^2}{m_t^2}, \frac{M_W^2}{m_t^2} \right) \xrightarrow{p_t^2 \rightarrow m_t^2} \text{const} \times \frac{1}{(m_t^2 - p_t^2)^2}$$

Linearly IR divergent. Finite in dim reg.

Equivalent to the dimensionally regulated $e^+e^- \rightarrow bW^+\bar{t}$ process with $\Gamma_t = 0$, expanded in the hard region around $s = 4m_t^2$.

Can impose invariant mass cuts on top decay products. $\Delta^2 = M_W^2$ for inclusive cross section. EFT works differently for loose and wide cuts [Actis, MB, Falgari, Schwinn, 2008]



QED and non-resonant corrections relative to the $t\bar{t}$ LO cross section in percent:
 $\sigma_{\text{QED}}^{(1)} / \sigma_{t\bar{t}}^{(0)}$ (upper solid blue), $\sigma_{\text{non-res}}^{(1)} / \sigma_{t\bar{t}}^{(0)}$ for the total cross section (lower solid red) and $\Delta M_t = 15$ GeV (lower dashed red). The relative size of the sum of the QED and non-resonant corrections is represented by the middle (black) lines, for $\Delta M_{t,\text{max}}$ (solid) and $\Delta M_t = 15$ GeV (dashed). $m_{t,\text{pole}} = 172$ GeV.

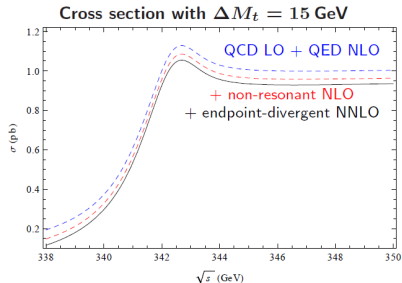
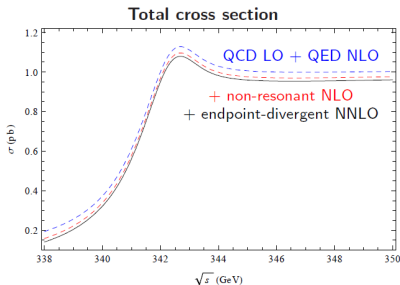
Large correction below threshold.

Much larger than QCD scale-dependence at 3rd order ($\pm(2 - 3)\%$)

$$e^+e^- \rightarrow W^+W^-b\bar{b} \text{ near } s = 4m_t^2$$

NLO + NNLO singular terms [Jantzen, Ruiz-Femenia, 2013; see also Hoang, Reisser, Ruiz-Femenia, 2010]

(Singular refers to expansion in Λ/m_t where Λ is an invariant mass cut such that $m_t\Gamma_t \ll \Lambda^2 \ll m_t^2$.)



NNLO non-resonant still -2% at threshold and larger below.

Accurate description of region below peak is required for precise determination of m_t .

- I $e^+e^- \rightarrow t\bar{t}X$ cross section near threshold now computed at NNNLO in (PNR)QCD
 - Sizeable 3rd order corrections and reduction of theoretical uncertainty.
 - Parameter dependences ($m_t, \Gamma_t, y_t, \alpha_s$) can be studied.

- II Realistic predictions for $e^+e^- \rightarrow W^+W^-b\bar{b}$ near top-pair threshold
 - NLO available, including cuts invariant mass cuts.
Should (and can) be done to NNLO. Residual uncertainty should then be small.
 - ISR should be done by theorists.
Known in principle, in practice accuracy may not yet be sufficient.

- III What is limiting the mass measurement: statistics? experimental systematics? theory? Still open.